Revista Brasileira de Meteorologia, Online Ahead of Print, 2022
DOI: http://dx.doi.org/10.1590/0102-77863730054

Spatial Distribution of Droughts in the Titicaca Lake Basin

Wendy A. Alonso[1], Waldo Lavado-Casimiro[2], Raúl Espinoza-Villar[1],
Eduardo Chávarri-Velarde[3]

[1]*Departamento de Ordenamiento Territorial y Construcción, Universidad Nacional Agraria La Molina, Lima, Perú.*
[2]*Servicio Nacional de Meteorología e Hidrología del Perú, Lima, Perú.*
[3]*Departamento de Recursos Hídricos, Universidad Nacional Agraria La Molina, Lima, Perú.*

Received: 7 February 2021 - Accepted: 8 February 2022

Abstract

The present research has assessed the spatial distribution of drought risk in the Titicaca Lake Basin located in Peruvian territory for a district scale, based on hazard and vulnerability. Drought hazard has been quantified with the deficit of precipitation using the Standardized Precipitation Index (SPI) for a time scale of 3-months, and the vulnerability has been obtained according to the socio-economic and physical indicators of the Basin. The results show that the drought is strongly modulated by anomalous SST conditions of the surrounding Oceans, mainly by the Pacific region. Over the Titicaca Lake Basin was identified that about 50% of districts present a high to very high risk of drought mainly, in the northwestern, central-east, and central-south of the Basin. These districts have a larger deficit of precipitation and showed indicators that are more vulnerable to the drought hazard due to that economically depends on precarious rainfed agriculture and an extensive and mixed livestock system. Within this area are the most important provinces of the high-Andean region, such as Puno, San Roman, Azángaro, Melgar, and Carabaya, and outstanding districts as Puno and Juliaca, considered the economic capital of the department of Puno.

Keywords: Titicaca Lake basin, drought, risk, hazard, vulnerability.

Distribuição Espacial das Secas na Bacia do Lago Titicaca

Resumo

A presente pesquisa avaliou a distribuição espacial do risco de seca na bacia hidrográfica do lago Titicaca localizada em território peruano para uma escala de distrito, com base em perigo e vulnerabilidade. O perigo foi quantificado com o déficit de precipitação usando Índice de Precipitação Padronizado (SPI, por suas siglas em inglês), para uma escala de tempo de três meses; e a vulnerabilidade foi obtida de acordo com os indicadores socioeconômicas e físicas da bacia. Os resultados mostram que a seca é fortemente modulada por condições anômalas de TSM dos oceanos circundantes, principalmente pela região do Pacífico. Na Bacia do Lago Titicaca, foi identificado que aproximadamente 50% dos distritos apresentam alto a muito alto risco de seca, localizados principalmente no Noroeste, centro-leste, e centro-sul da bacia. Esses distritos apresentam um maior déficit de precipitação e apresentam indicadores mais vulneráveis ao perigo de seca devido ao facto de depender economicamente de uma agricultura de sequeiro precária e de um sistema de pecuária extensiva e mista. Nesta área estão as províncias mais importantes da região alto-andino, como Puno, San Roman, Azángaro, Melgar e Carabaya, e destacam-se distritos como Puno e Juliaca considerado o capital econômico do departamento de Puno.

Palavras-chave: Bacia hidrográfica do lago Titicaca, seca, risco, perigo, vulnerabilidade.

1. Introduction

Drought is one of the most damaging natural hazards related to climate (Sönmez *et al.*, 2005), and is considered to affect more people than any other natural disaster on the planet (Ortega, 2013). It is therefore considered by many to be the most complex but least understood of all-natural hazards (WMO, 2016). It differs from other hazards such as floods, tropical cyclones, and earthquakes because it builds up slowly over a considerable period and can per-

Autor de correspondência: Wendy A. Alonso, waramayo@lamolina.edu.pe.

sist for years after the event has ended, making it difficult to determine the beginning and end (Tannehill, 1947).

Usually, droughts are classified according to type, in meteorological, agricultural, and hydrological, and they are differentiated by their intensity, duration, and spatial extent (OMM, 2012). Meteorological drought is defined as a threshold of precipitation deficit that is reached during a period previously determined (OMM, 2006). The majority of available drought-related indices focus on the assessment of meteorological drought, for example, Standard Precipitation Index (SPI), Palmer Index (PI), Simple Precipitation Intensity Index (SPII) (Rojas, 2021). The index most used is the Standardized Precipitation Index (SPI), which is recommended by the World Meteorological Organization (WMO) as the standard drought index (Serafini *et al.*, 2019) given its simplicity and flexibility for the study of precipitation on various time scales (Endara *et al.*, 2019). Mckee *et al.* (1993) originally developed the SPI to quantify the precipitation deficit, for different time scales of 3, 6, 12, 24, and 48 months. Short-term scales such as months may be important for agricultural interests, while long-term scales such as years may be transcendental for interests in water supply management (Guttman, 1998).

In Peru, the droughts are quite often since last decades, according to Lovón (1985). Between 2000 and 2010, 163 drought events with different frequencies were reported at the national level, being higher on the Basin of Pacific, followed by the Titicaca Lake Basin (ANA, 2013). The Titicaca Lake Basin is located in the southern region of Peru, an area where several drought events have occurred (Vega, 2016). According to the National Institute of Civil Defense (INDECI, by acronym in Spanish), historically the area of the southern highlands of Peru is the area most prone to the occurrence of droughts, this area includes the departments of Puno, Cusco, Tacna, Moquegua, Arequipa and Apurimac, with 70% of the population economically active in rainfed agriculture and livestock. One of the most critical occurred at the end of 1982 and the beginning of 1983, it was an exceptional drought that fundamentally affected the highland the Puno and Cusco departments (Lovón, 1985).

The Lake Titicaca Basin region features several characteristics that influence the spatial-temporal rainfall distribution, and many studies have shown that regions with lakes (e.g., Lake Titicaca Basin) are affected by a combination of orographic and convective precipitation (Chuchón and Pereira, 2022). The rainy season over the Altiplano occurs during the austral summer linked to the active phase of the South America Monsoon System-SAMS (Zhou and Lau 1998; Vera *et al.*, 2006). The peak of precipitation occurs in January, and is characterized by intense convective activity combined with moisture advection from the Amazon Basin (Aceituno and Montecinos 1993; Chaffaut *et al.*, 1998; Vuille *et al.*, 1998; Garreaud *et al.*, 2003; Vizy and Cook, 2007; Mayta *et al.*, 2019). During the austral winter (in the absence of the SAMS influence), the moist eastern flux is replaced by westerly winds, which provide dry air related to the atmospheric stability over the Pacific Ocean. This strong seasonality explains that almost all precipitation occurs in 1-3 month (Lavado *et al.*, 2012).

The present research assesses the spatial distribution of drought risk in the Titicaca Lake Basin located in Peruvian territory for a district territorial division, based on hazard and vulnerability. The drought hazard is estimated with the precipitation deficit monthly rainfall obtained from the latest version of product PISCO - Precipitation v1.2 (Peruvian Interpolation of the SENAMHIs Climatological and Hydrological Stations) for the period 1981 to 2016 (36 years), and then is quantified with the Standardized Precipitation Index (SPI) for a time scale of 3-months. The vulnerability is obtained according to socio-economic and physical indicators of the hydrographic Basin of Lake Titicaca.

1.1. Geographical and climatic characteristics of the Titicaca Lake basin

The hydrographic Basin of Lake Titicaca is located in South America, south of Peru and northwest of Bolivia, between 14°05' and 16°50' north longitude and 68°10' and 71°05' west longitude, on the Peruvian territory covers an area of 48,910 km^2 including the part corresponding to the Lake, with an altitude varying between 3,812 and 5,500 m.a.s.l. In addition, has a cold and dry climate, with a maximum temperature of 18 °C, a minimum of -2 °C, and an average of 10 °C. The spatial distribution of annual mean precipitation has a decreasing pattern from north to south. In general, it varies from 200 to 1,400 mm (INEI, 2013).

In Peruvian territory, the Titicaca Lake Basin is located within the high-Andean region of the department of Puno, occupying approximately 63% of its surface. This is composed of 13 provinces and 90 districts, as can be seen in Fig. 1 and listed in Table 1. The district with the largest area is Santa Rosa district with 2,472 km^2, belonging to the province of El Collao, followed by Nuñoa district with 2,209 km^2, located in the province of Melgar. Likewise, the Titicaca Lake Basin is made up of 16 hydrographic units, as can be seen in Fig. 2. The hydrographic unit of Azángaro has the largest area with 8,754 km^2, followed by the Pucará with 5,541 km^2.

2. Data and Methodology

2.1. Data

2.1.1. Precipitation data

Monthly rainfall is obtained from product PISCO-Precipitation v1.2 (Peruvian Interpolation of the SENAMHIs Climatological and Hydrological Stations) for the per-

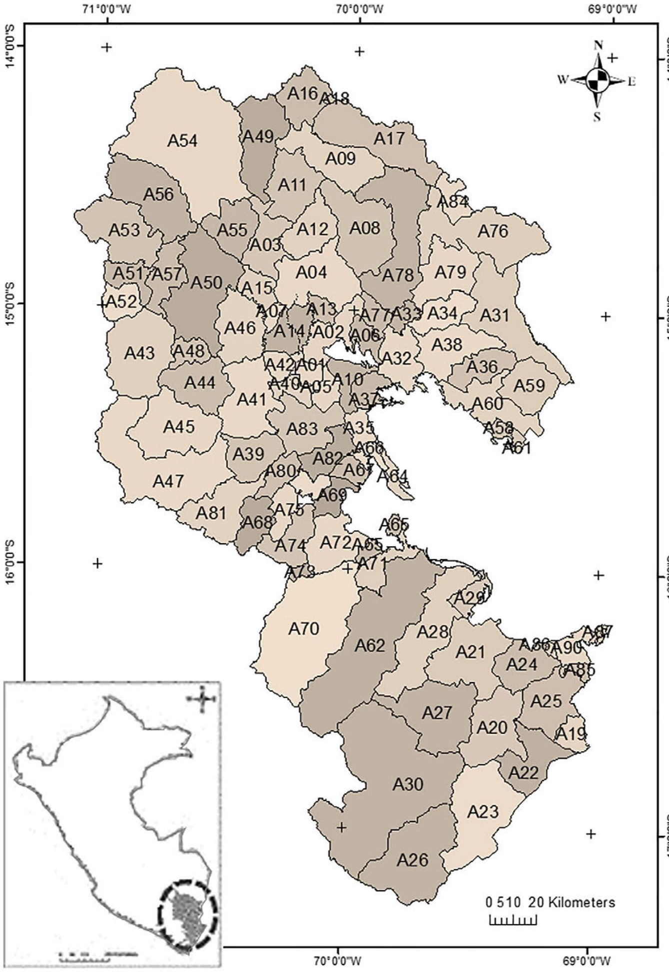

Districts in the Titicaca Lake Basin					
A01	Achaya	A31	Cojata	A61	Tilali
A02	Arapa	A32	Huancané	A62	Acora
A03	Asillo	A33	Huatasani	A63	Atuncolla
A04	Azángaro	A34	Inchupalla	A64	Capachica
A05	Caminaca	A35	Pusi	A65	Chucuito
A06	Chupa	A36	Rosaspata	A66	Coata
A07	José Domingo Choquehuanca	A37	Taraco	A67	Huata
A08	Muñani	A38	Vilque Chico	A68	Mañazo
A09	Potoni	A39	Cabanilla	A69	Paucarcolla
A10	Saman	A40	Calapuja	A70	Pichacani
A11	San Antón	A41	Lampa	A71	Plateria
A12	San José	A42	Nicasio	A72	Puno
A13	San Juan de Salinas	A43	Ocuviri	A73	San Antonio
A14	Santiago de Pupuja	A44	Palca	A74	Tiquillaca
A15	Tirapata	A45	Paratia	A75	Vilque
A16	Ajoyani	A46	Pucara	A76	Ananea
A17	Crucero	A47	Santa Lucia	A77	Pedro Vilca Apaza
A18	Usicayos	A48	Vilavila	A78	Putina
A19	Desaguadero	A49	Antauta	A79	Quilcapuncu
A20	Huacullani	A50	Ayaviri	A80	Cabana
A21	Juli	A51	Cupi	A81	Cabanillas
A22	Kelluyo	A52	Llalli	A82	Caracoto
A23	Pisacoma	A53	Macari	A83	Juliaca
A24	Pomata	A54	Nuñoa	A84	Cuyocuyo
A25	Zepita	A55	Orurillo	A85	Copani
A26	Capazo	A56	Santa Rosa	A86	Cuturapi
A27	Conduriri	A57	Umachiri	A87	Ollaraya
A28	Ilave	A58	Conima	A88	Tinicachi
A29	Pilcuyo	A59	Huayrapata	A89	Unicachi
A30	Santa Rosa	A60	Moho	A90	Yunguyo

Figure 1 - The Titicaca Lake Basin located in Peruvian Territory at the district scale.

iod 1981 to 2016 (36 years). PISCO - precipitation is a spatial precipitation database produced and validated by the National Meteorological and Hydrological Service of Peru (SENAMHI, by acronym in Spanish) at a monthly time step and a grid resolution of 0.05°. The series starts in January 1981 until 2016 (Aybar *et al.*, 2017) and can be freely downloaded through the SENAMHI website. The validation of PISCO-precipitation in the hydrographic regions of Peru is detailed by Endara (2017) and Porto (2021).

2.1.2. Oceanic indices

To assess the impacts of El Niño-Southern Oscillation (ENSO) in precipitation, we used the eastern (E) and central (C) index which represent anomalous surface warming in the east and center Pacific, as can be seen in Fig. 3 documented in detail by Takahashi *et al.* (2011) and is available at the Climate Monitoring Indices of the Geophysical Institute of Peru. In addition, to measure the impacts of the anomalous condition over Tropical North Atlantic (TNA), we used the TNA index. This index is computed as the anomaly of the average of the monthly SST over 55° W-15° W, 5° N-25° N region and is available from NOAA Climate Indices.

2.1.3. Socioeconomic and physical indicators

The indicators were quantified using the latest National Censuses 2017: Population XII, Housing VII, and Indigenous Communities III; National Agricultural Census IV - 2012. Additionally, the Census population, statistical information of Economically Active Population, and Human Development Index are obtained from websites and can be freely downloaded.

2.2. Methodology

2.2.1. Precipitation analysis

The rainy months are identified for drought monitoring in the Titicaca Lake Basin due to that the main economic activities in the Basin depend on rainfall for their development. The fluctuation of the rainy months and their slope-index are calculated to know if increase or decrease the precipitation trends, and detect if they present statistical significance. The trend analysis was carried out with the statistical test non-parametric Mann-Kendall at a 95% of confidence level.

Table 1 - Provinces and Districts on the Titicaca Lake Basin located in Peruvian Territory.

Azángaro Province composed of the following districts:		
A01	Achaya	127.15 km^2
A02	Arapa	338.04 km^2
A03	Asillo	405.52 km^2
A04	Azángaro	724.22 km^2
A05	Caminaca	146.67 km^2
A06	Chupa	152.92 km^2
A07	José Domingo Choquehuanca	67.25 km^2
A08	Muñani	788.72 km^2
A09	Potoni	625.62 km^2
A10	Saman	204.79 km^2
A11	San Antón	518.23 km^2
A12	San José	399.34 km^2
A13	San Juan de Salinas	105.18 km^2
A14	Santiago de Pupuja	320.47 km^2
A15	Tirapata	201.65 km^2
Carabaya Province composed of the following districts:		
A16	Ajoyani	385.54 km^2
A17	Crucero	858.88 km^2
A18	Usicayos	14.71 km^2
Chucuito Province composed of the following districts:		
A19	Desaguadero	162.26 km^2
A20	Huacullani	632.24 km^2
A21	Juli	778.17 km^2
A22	Kelluyo	486.70 km^2
A23	Pisacoma	958.76 km^2
A24	Pomata	404.24 km^2
A25	Zepita	527.55 km^2
El Collao Province composed of the following districts:		
A26	Capazo	1,048.26 km^2
A27	Conduriri	850.62 km^2
A28	Ilave	895.13 km^2
A29	Pilcuyo	153.22 km^2
A30	Santa Rosa	2,472.45 km^2

Huancané Province composed of the following districts:		
A31	Cojata	885.50 km^2
A32	Huancané	389.32 km^2
A33	Huatasani	106.89 km^2
A34	Inchupalla	298.75 km^2
A35	Pusi	147.28 km^2
A36	Rosaspata	307.61 km^2
A37	Taraco	197.09 km^2
A38	Vilque Chico	511.83 km^2
Lampa Province composed of the following districts:		
A39	Cabanilla	386.78 km^2
A40	Calapuja	143.05 km^2
A41	Lampa	663.87 km^2
A42	Nicasio	133.93 km^2
A43	Ocuviri	869.62 km^2
A44	Palca	497.14 km^2
A45	Paratia	750.66 km^2
A46	Pucara	527.98 km^2
Lampa Province composed of the following districts:		
A47	Santa Lucia	1,381.93 km^2
A48	Vilavila	161.80 km^2
Melgar Province composed of the following districts:		
A49	Antauta	658.23 km^2
A50	Ayaviri	1,021.73 km^2
A51	Cupi	217.50 km^2
A52	Llalli	221.64 km^2
A53	Macari	693.31 km^2
A54	Nuñoa	2,208.76 km^2
A55	Orurillo	399.26 km^2
A56	Santa Rosa	806.45 km^2
A57	Umachiri	333.11 km^2
Moho Province composed of the following districts:		
A58	Conima	67.70 km^2
A59	Huayrapata	405.49 km^2
A60	Moho	507.83 km^2
A61	Tilali	51.30 km^2

Puno Province composed of the following districts:		
A62	Acora	1,925.01 km^2
A63	Atuncolla	131.29 km^2
A64	Capachica	104.03 km^2
A65	Chucuito	115.84 km^2
A66	Coata	99.88 km^2
A67	Huata	129.17 km^2
A68	Mañazo	280.54 km^2
A69	Paucarcolla	174.39 km^2
A70	Pichacani	1,644.94 km^2
A71	Plateria	243.94 km^2
A72	Puno	462.69 km^2
A73	San Antonio	42.69 km^2
A74	Tiquillaca	345.09 km^2
A75	Vilque	195.83 km^2
San Antonio de Putina Province composed of the following districts:		
A76	Ananea	970.92 km^2
A77	Pedro Vilca Apaza	143.65 km^2
A78	Putina	1,043.07 km^2
A79	Quilcapuncu	527.70 km^2
San Román Province composed of the following districts:		
A80	Cabana	193.94 km^2
A81	Cabanillas	552.15 km^2
A82	Caracoto	282.31 km^2
A83	Juliaca	533.99 km^2
Sandia Province composed of the following districts:		
A84	Cuyocuyo	190.03 km^2
Yunguyo Province composed of the following districts:		
A85	Copani	59.25 km^2
A86	Cuturapi	23.92 km^2
A87	Ollaraya	26.73 km^2
A88	Tinicachi	3.62 km^2
A89	Unicachi	5.92 km^2
A90	Yunguyo	175.97 km^2

2.2.2. Drought hazard calculation

The precipitation deficit of meteorological drought in the Titicaca Lake Basin is quantified using the Standardized Precipitation Index (SPI) for a temporary scale of 3-months. The short time scales (1, 2, or 3 months), can provide an early warning of drought and help assess drought severity (OMM, 2012). In the Titicaca Lake Basin, it can be essential because the agricultural activity is the primary source of economic income in the region and it depends on the precipitation for its development. Table 2 shows the category of droughts defined by SPI values. There is evidence that the high-Andean region of Puno presents a strong signal associated with anomalous conditions observed in the Pacific region (i.e., El Niño). Therefore, the correlation between the Peruvian precipitation (from PISCO for January to March season and the 1980-2016 period) against the TNA index, E index, and C index is analyzed.

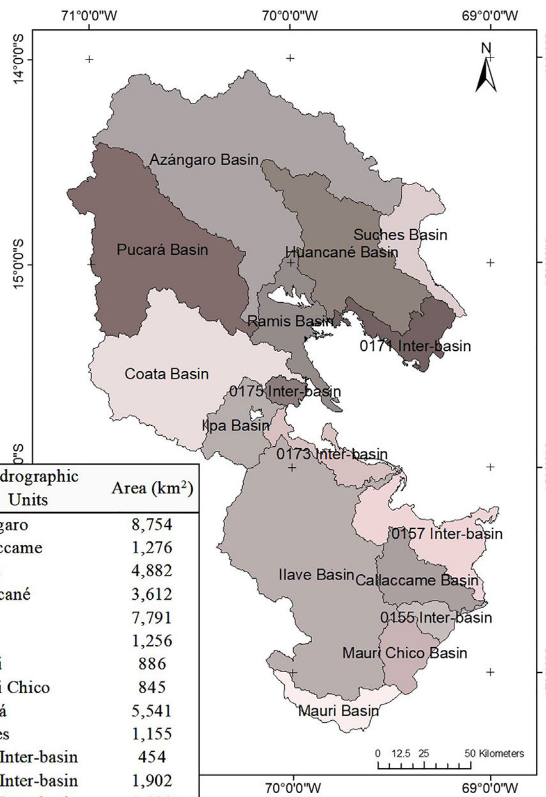

Hydrographic Units	Area (km²)
Azángaro	8,754
Callaccame	1,276
Coata	4,882
Huancané	3,612
Ilave	7,791
Ilpa	1,256
Mauri	886
Mauri Chico	845
Pucará	5,541
Suches	1,155
0155 Inter-basin	454
0157 Inter-basin	1,902
0171 Inter-basin	1,020
0173 Inter-basin	804
0175 Inter-basin	279
Ramis Inter-basin	1,575

Figure 2 - Hydrographic Units of the Titicaca Lake Basin located in Peruvian Territory.

For the calculation of drought hazard, each district is assigned a weight and a rating using the analytical hierarchy process (AHP), according to the drought category (moderate, severe, or extreme) that depends on the values obtained from the SPI and the percentage of drought occurrence. AHP is a decision-making method that systematically evaluates alternatives to derive priorities and importance when evaluation criteria are numerous and complex (Young-Sik *et al.*, 2020). The percentage of drought occurrence is calculated by dividing the number of specific drought events (moderate, severe, or extreme) by the total events of the analyzed period. Table 3 shows the weights and qualifications assigned according to drought category and percentage of drought occurrence.

The drought occurrence and hazard maps are developed for a time scale of 3-months at the district scale. The maps are made using the kriging interpolation method which is widely recognized as a standard approach for interpolating surfaces based on scalar measurements of

Table 2 - Category of droughts defined by SPI values.

SPI value	Drought category	Probability of occurrence (%)
0.00 a - 0.99	Slight drought	~ 24
-1.00 a -1.49	Moderate drought	9.2
-1.50 a -1.99	Severe drought	4.4
≤ -2.00	Extreme drought	2.3
		~ 40

Source: McKee *et al*. (1993).

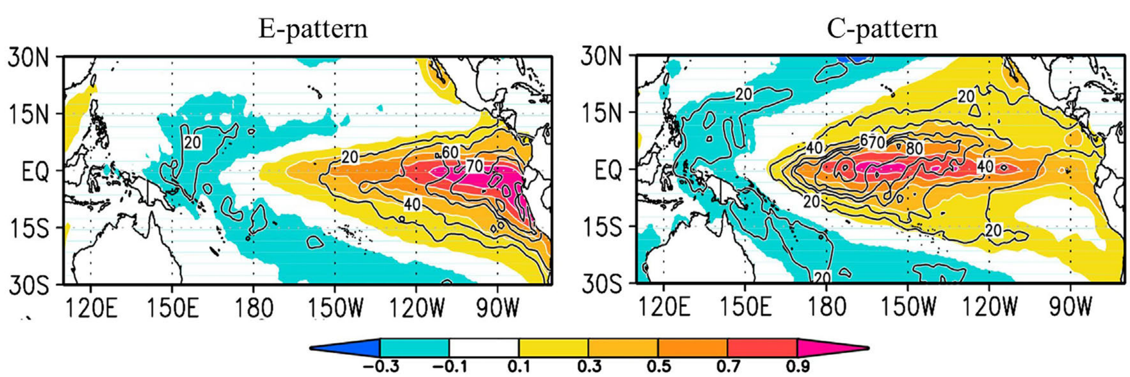

Figure 3 - The patterns of sea surface temperature anomalies associated with unit values of the E-index, and the C-index. Source: Takahashi *et al.* (2011).

Table 3 - Weights and qualifications are assigned according to drought category and PO.

Drought category	Weights	Percentage of drought occurrence (PO)	Qualification
Moderate	1.0	≤ 9.0	1.0
		9.1 - 10.0	2.0
		10.1 - 11.0	3.0
		≥ 11.1	4.0
Severe	2.0	≤ 3.5	1.0
		3.6 - 4.5	2.0
		4.6 - 5.5	3.0
		≥ 5.6	4.0
Very severe	3.0	≤ 1.5	1.0
		1.6 - 2.0	2.0
		2.1 - 2.5	3.0
		≥ 2.6	4.0

Source: Shahid and Behrawan (2008).

different points (Shahid and Behrawan, 2008). The Drought Hazard Index (DHI) was derived using Eq. (1) according to Hungsoo *et al.* (2015).

$$DHI = (MDw \times MDr) + (SDw \times SDr) + (VSDw \times VSDr) \quad (1)$$

where *MDw* is the weight assigned to moderate drought; *MDr* is rating assigned to the moderate drought percentage of drought occurrence; *SDw* is the weight assigned to severe drought; *SDr* is rating assigned to the severe drought percentage of drought occurrence; *VSDw* is the weight assigned to extreme drought; *VSDr* is rating assigned to the extreme drought percentage of drought occurrence.

2.2.3. Vulnerability to drought calculation

The vulnerability to drought is obtained by Eq. (2), which is based on 4-socioeconomic and 2-physical indicators of the Titicaca Lake Basin. The Titicaca Lake Basin is located within the high-Andean region of the department of Puno, which is one of the departments with more poverty at the national level, with main economic activities that depend on the rains for their development such as rainfed agriculture and livestock. For this reason, the socioeconomic and physical indicators are chosen according to the most relevant activities and characteristics of the region which are negatively affected due to the impact of drought events. Table 4 shows the socioeconomic and physical indicators detailed.

The socioeconomic and physical indicators are divided into 4 classes: low, moderate, high, and very high, using the natural breaks method (Jenks). The natural break method is used to derive the classes. This method creates a range according to an algorithm that uses the average of each range to distribute the data more evenly across the ranges (Shahid and Behrawan, 2008). This method ensures that the ranges are well represented by their averages and that the data values within each range are fairly close together (Smith, 1986). GIS software ArcView 9.0 is used to identify the natural breakpoints in the data.

The vulnerability to drought is obtained with the index that is the average of the scores assigned to each indicator as shown in the Eq. (2) according to Johnson *et al.* (2016). The vulnerability index is classified into four ranges with the Natural Break method (Jenks), according to their 25%, 50% and 75% percentiles, then scores of 1.0, 2.0, 3.0 and 4.0 are placed to distinguish their levels of vulnerability (low, moderate, high and very high). Finally, the drought vulnerability map is prepared at the district level differentiated the vulnerability levels with colors.

$$DVI = \frac{(Dp + Id + Ae + Rhm + Pg + Da)}{\text{Number of indicators}} \quad (2)$$

where *Dp* is the score assigned to population density; *Id* is the score assigned to the Human Development Index; *Ae* is the score assigned to Active Economic Activity in agriculture, livestock, hunting, and forestry; *Rhm* is the score assigned to the female/male relation; *Pg* is the score assigned to the livestock population; *Sa* is the score assigned to the rainfed agricultural area.

2.2.4. Drought risk calculation

Drought risk is obtained through the Drought Risk Index (DRI) which is a function of hazard and vulnerability, as shown by Eq. (3) according to Shahid and Behrawan (2008).

$$DRI = DHI \times DVI \quad (3)$$

Table 4 - Socioeconomic and physical indicators.

Socioeconomic indicator	Population Density: The number of people per unit area and is usually expressed in inhabitants per km^2.Human Development Index (IDH): It is calculated by the United Nations Development Programme (PNUD). Its levels range to go from 0 to 1. The factors taken into account to measure it are the average annual income per person, access to education and health services, and life expectancy.Economically Active Population (PEA) in Agriculture, Livestock, Hunting and Forestry: Represents the percentage of people who depend mainly on agriculture and livestock, as well as hunting and forestry.Female / Male relation: Represents the relation of female to male residents in a region. According to the Intergovernmental Panel on Climate Change (IPCC), women are more affected by the climate crisis than men.
Physical indicator	Livestock Production: The amount of livestock production in a region: alpacas, sheep, cattle, pigs, and other species.Rainfed Agricultural: Represents the agricultural area in hectares under rainfed irrigation. This indicator is highly vulnerable to drought events, due to the crops only receive the water provided by rainfall.

where *DRI* is the drought risk index; *DHI* is the drought hazard index; *DVI* is the drought vulnerability index. Figure 4 shows the schematic depiction of the methodology used in this study to calculate the drought risk.

3. Results and Discussion

3.1. Precipitation analysis

Figure 5 shows the spatial distribution of the annual mean precipitation (1981-2016) in the hydrographic units of the Titicaca Lake Basin and the rainfall for the January to March period. The precipitation over the Titicaca plateau is important to study because the development of the main industries in this region depends on it (Romero, 2013). The hydrographic units with the highest rainfall are located in the west, center, and east of the Titicaca Lake Basin, while those in the north and south show the lowest rainfall. The rainy months are January, February, and March (hereafter, JFM) due to during this period the precipitation is higher compared to the rest of the year, representing more than 50% of the annual accumulated precipitation. July is the driest month, while January is the wettest month (Andrade, 2017). During the JFM season, the hydrographic units located in the southern and eastern of the Basin show fluctuation and slope-index negative, which indicates decrease precipitation concerning the average. These Basins are Huancané, Ilave, Suches, Callaccame, Mauri Chico, and the Inter-Basins of 0157, 0173, 0171, 0155, 0175, and Ramis. Ramis shows the lowest slope-index with -0.052, followed by the Huancané with -0.033. In contrast, the hydrographic units located in the north and west show fluctuation and slope-index positives, which indicates an increase in the precipitation concerning the average. The trend analysis from the Mann-Kendall test on the rainfall with a 95% of confidence level not show statistical significance in any period of the time series analyzed.

3.2. Drought hazard

Figure 6 shows the districts with the highest fluctuation of the Standardized Precipitation Index (SPI) for a time scale of 3-months in the period 1981 to 2016. In the Fig. 6.a the 3-months SPI for rainy season (JFM) is analyzed and not the winter period because a significant dry period during the winter season may have few impacts (Wilhite, 2000). During JFM is not detected significant changes in the SPI fluctuation, so not show statistical significance in any period of the time series analyzed. In 1983, 1987, 1990 and 1992, occurred extreme ($SPI \leq -2.00$), severe ($-1.50 \leq SPI \leq -1.99$) and moderate ($-1.0 \leq SPI \leq -1.49$) drought events with categories and intensities different. The longest extreme drought occurring in 1983 with a period of 60 days, while the severe droughts in 1990 and 1992 lasted 37 and 40 days. The SPI reached values of -3.76 in 1983 in Vilavila district; -2.82 in 1990 in Antauta district; -2.69 in 1987 in Orurillo

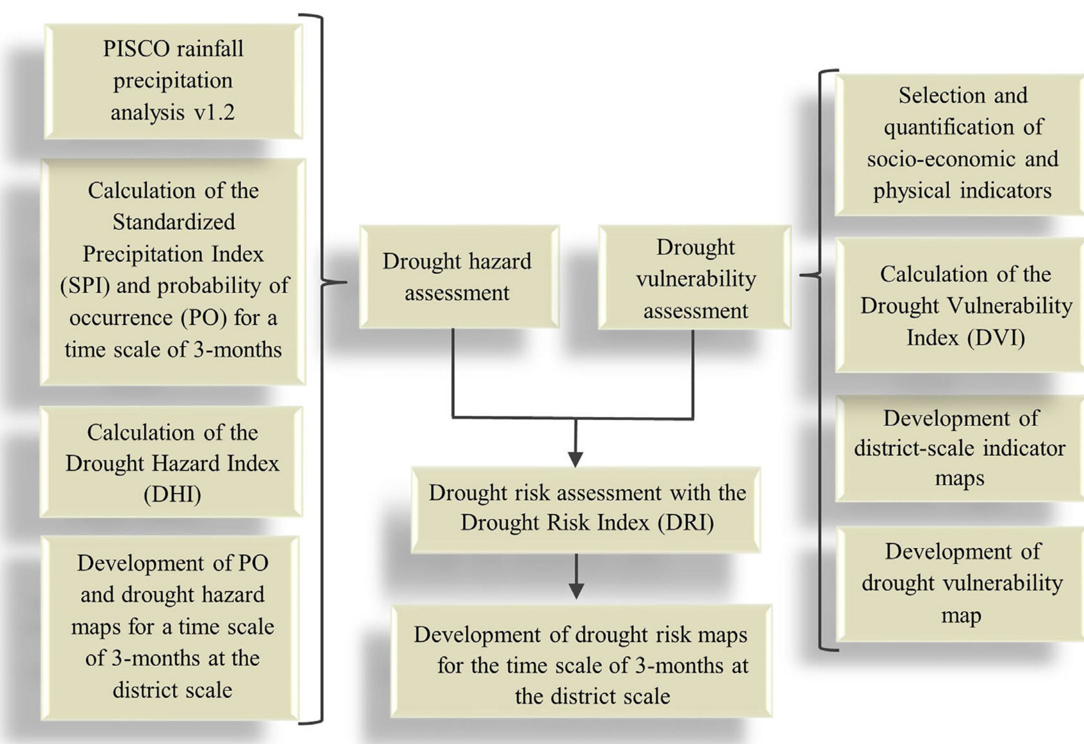

Figure 4 - Schematic depiction of the methodology used in this study.

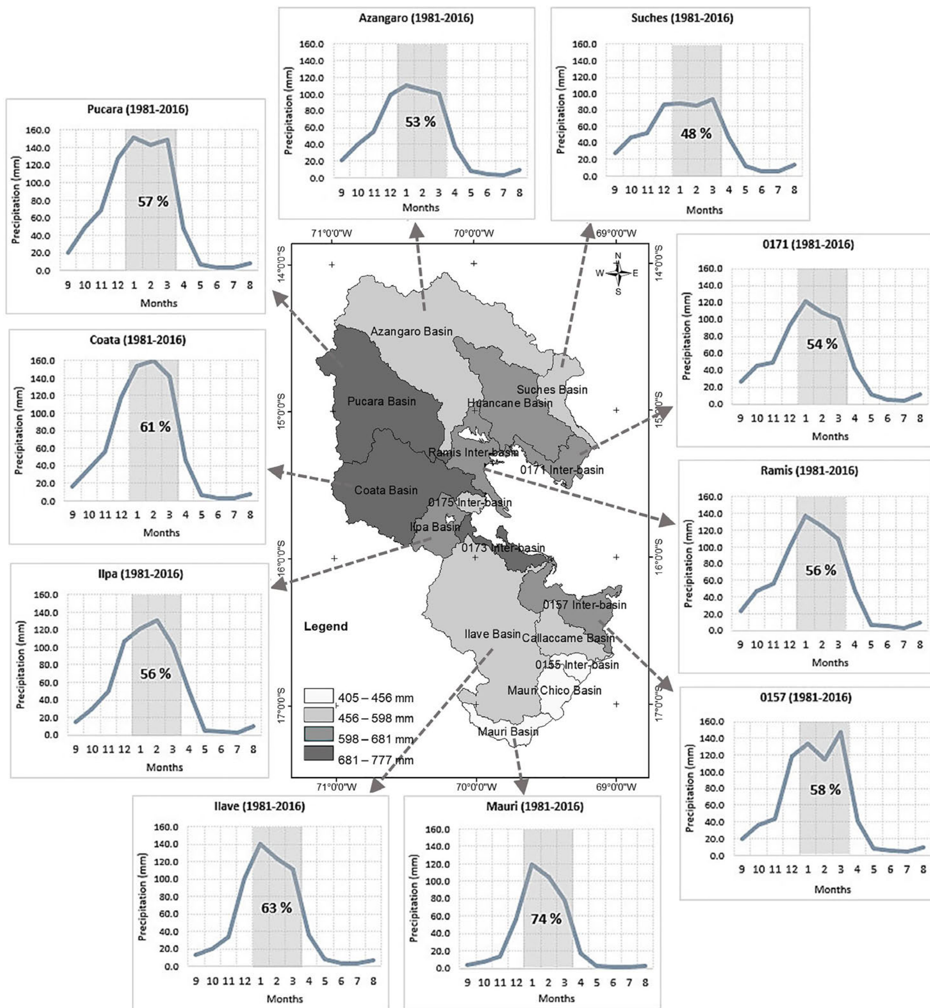

Figure 5 - Spatial distribution of the annual mean precipitation (1981-2016) in the hydrographic units of the Titicaca Lake Basin and the rains of January, February, and March (JFM).

district and -2.62 in 1992 in San Antonio district. Severe and moderate droughts were detected in 1982, 1989, 1998, 2005, 2006, 2009 and 2016 in districts of the high-Andean region of Puno, and only moderate drought were observed in 1988, 1991, 1993, 1995, 1996, 2000, 2003, 2008, 2010, 2011, 2013, 2014 and 2015. According to ANA (2013), the drought event in 2011 affected various departments, such as Arequipa, Cajamarca, Lambayeque, Piura, La Libertad, Lima, Moquegua, Tacna, Amazonas, Huánuco, San Martín, Junín and Puno. The drought recorded in 1982-83 resulted from a rainfall deficit during El Niño conditions (analyzed in next section) when upper-level west wind anomalies inhibited the influx of moisture from the east (Sulca *et al.*, 2018), causing losses in the Puno region in agriculture that were much larger than in livestock (Claverías, 2016). Likewise, in 1992 drought coincidentally occurred with El Niño year and was the most severe and affected 16 departments in Peru: Amazonas, Cajamarca, La Libertad, Ancash, Junín, Huánuco, Huancavelica, Pasco, Lima, Cusco, Apurímac, Ayacucho, Arequipa, Tacna, Moquegua and Puno (Endara *et al.*, 2019). On the other hand, it should be noted that in 1983 and 1992 droughts followed a volcanic eruption in the Tropic, El Chichón in April 1982 in Mexico, and Mt. Pinatubo in June 1991 in the Philippines (Imfeld *et al.*, 2019).

Figure 6.b shows the precipitation deficit analyzed with the 3-months SPI in every month of the year, finding 59 districts out of 90 (59/90) present negative fluctuation and 31/90 districts present positive fluctuation for the period 1981 to 2016. In the analysis of the SPI, it has been registered 19,317 drought events during the period from 1981 to 2016, of which: 68% (13,074) is slight drought; 18% (3,535) is moderate drought; 9% (1,788) is severe drought, and 5% (920) is extreme drought.

According to Caviedes (1973), ENSO and drought are indeed the consequence of the same large-scale variation in the tropical and equatorial circulation, and that the

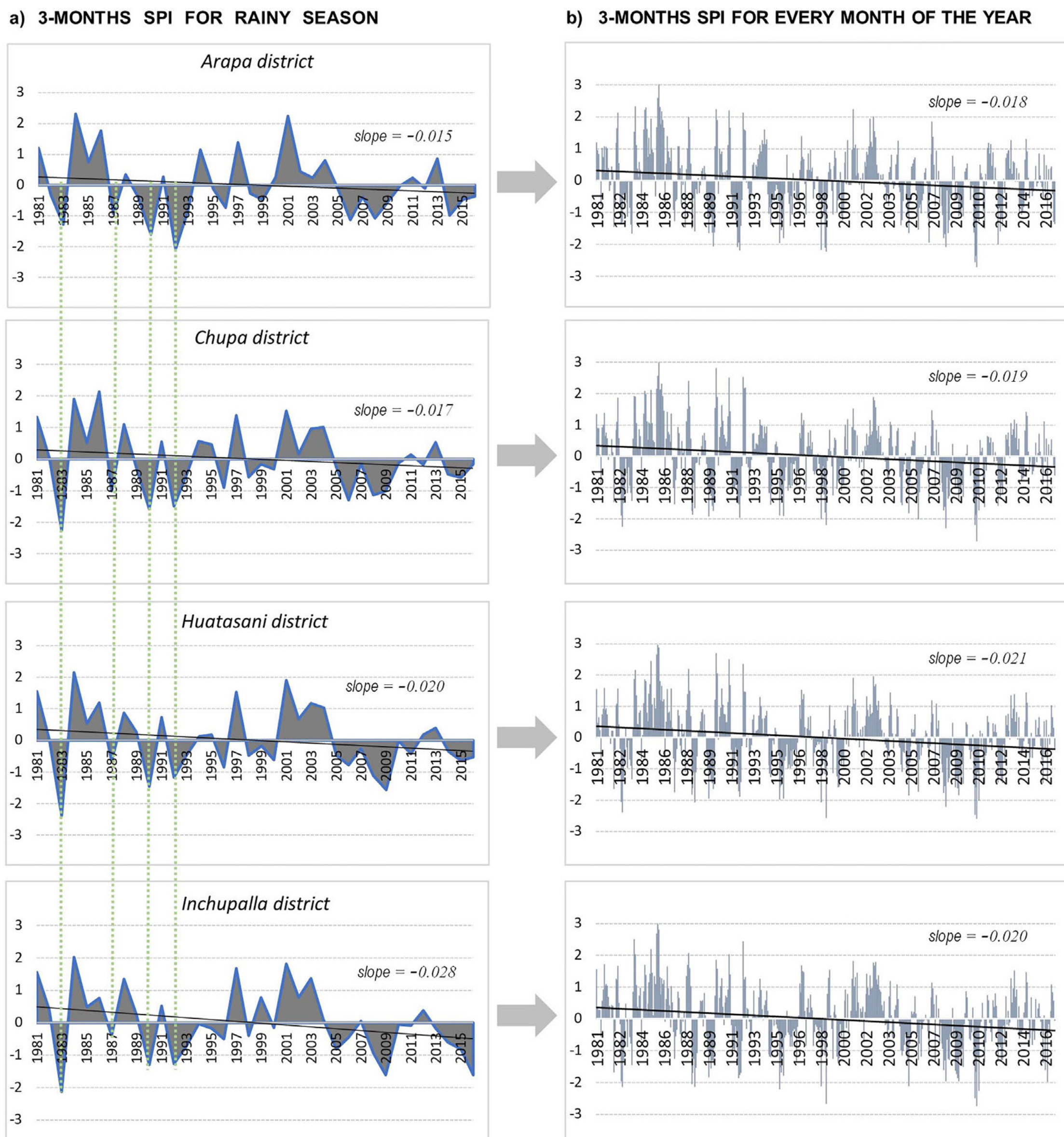

Figure 6 - Districts with the highest fluctuation of the Standardized Precipitation Index (SPI) for a time scale of 3-months in the 1981 to 2016 period.

closeness of the years of their occurrence is not just a coincidence. The climate of South America (SA) has long held an intimate connection with El Niño (Cai *et al.*, 2020). The main climate anomalies that characterize the El Niño in South America are related to a modification of the Walker circulation and to a southern shift of the Intertropical Convergence Zone, they include manifestation of the significant rainfall deficits in the Altiplano of southeastern Peru and Bolivia, the Brazilian northeastern, northtern of South America and southern of Central America (Ortlieb and Macharé, 1993). In Peru, El Niño phenomenon mainly generates climatic alteration that is manifested in intense rains in the north and severe droughts in the altiplano region of the south (Fig. 7) where is the hydrographic drainages of Lake Titicaca that present a significant rainfall deficit during the El Niño phenomenon (Lagos *et al.*, 2008; Lavado and Espinoza 2014).

Figure 7 shows the correlation between PISCO-precipitation for the JFM season and the C, E, and TNA index. Precipitation extremes in the southern Andean region are highly impacted by SST anomalous conditions in the central and eastern Pacific, showing negative correlations (precipitation deficit) (Figs. 7.b and 7.c). On the other hand, impacts of anomalous conditions in the tropical Atlantic, during the rainy season, is barely detected (Fig. 7.a). These results are in agreement with findings observed in Fig. 6, where SPI peaks (positive and negative) are strongly associated with El Niño and La Niña events recorded in recent decades. Table 5 shows ENSO influence on hydrographic units of the Titicaca Lake Basin through the E (eastern El Niño) and C (central El Niño) index based on Fig. 7. Table 1 shows the districts that are within the hydrographic units. The Basins of Azángaro, Callaccame, Coata, Ilave, Ilpa, Mauri, Mauri Chico, Pucará and Inter-Basins of 0155, 0157, 0173, 0175, present a very strong correlation with the C index which indicates correlation with cold, moderately-warm, and neutral events in the central Pacific, and the Basin of Huancané presented more correlation with the E index, which indicates warm events in the equatorial Pacific.

Figure 8 shows the probability of drought occurrence (PO) in drought categories: moderate, severe, and extreme, in the districts of the Titicaca Lake Basin. The PO levels are low, moderate, high, and very high, and according to each category of drought, the following has been found:

- Moderate drought: In this category are 23 districts out of 90 (23/90) that present very-high PO; 26/90 have high PO; 23/90 maintain a moderate PO and 18/90 have a low level of PO. The districts with high to very-high PO are located in the northeast, central, and southeast of the Titicaca Lake Basin, covering 54% of the Basin.
- Severe drought: In this case, show 23 districts out of 90 (23/90) that present very-high PO; 25/90 have high PO; 22/90 maintain a moderate PO and 20/90 have a low level of PO. The districts with high to very-high PO are located in the north, west, and south-east, and represent 49% of the Basin.
- Extreme drought: In this analysis, it has been found that 27 districts out of 90 (23/90) present very-high PO; 26/90 have high PO; 17/90 maintain a moderate PO and 20/90 have a low level of PO. The districts with high to very-high PO are located in the northwest, northeast, and center-south, and covers 68% of the Basin.

Figure 9 shows the drought hazard of the Titicaca Lake Basin, at the district scale for a time scale of 3-months SPI (in every month), obtained using Table 3. The results suggest that 37 districts out of 90 (37/90) show very-high drought hazard, 9/90 districts present high hazard, and 24/90 show moderate hazard. The districts with a high degree of exposure to drought events (high to very-high hazard) predominate in the northeast and center-south of the Titicaca Lake Basin, covering 51% of the area. In addition, the districts located in the part of the center-north and south of the Basin show low to moderate risk except for Capazo district. The drought hazard is caused by the precipitation deficit that can be associated with the occurrence of special climatic conditions.

Table 5 - ENSO influence on hydrographic units of the Titicaca Lake Basin through the E (eastern El Niño) and C (central El Niño) index based on Fig. 7.

Hydrografic units	C/E indices
Azángaro	C
Callaccame	C
Coata	C
Huancané	E
Ilave	C
Ilpa	C
Mauri	C
Mauri Chico	C
Pucará	C
Suches	-
Interc. 0155	C
Interc. 0157	C
Interc. 0171	-
Interc. 0173	C
Interc. 0175	C
Interc. Ramis	-

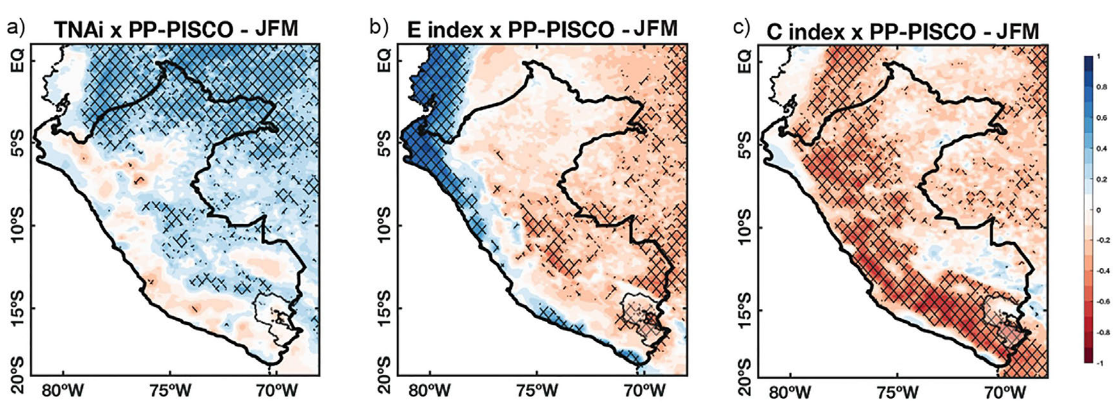

Figure 7 - Correlation between the Peruvian precipitation against the (a) TNA index, (b) E index, and (c) C index. Precipitation data comes from PISCO for January to March season and the 1980-2016 period. Blue (red) shadings indicate positive (negative) correlation, where statistically significant values (95% of confidence level) are plotted in hatching.

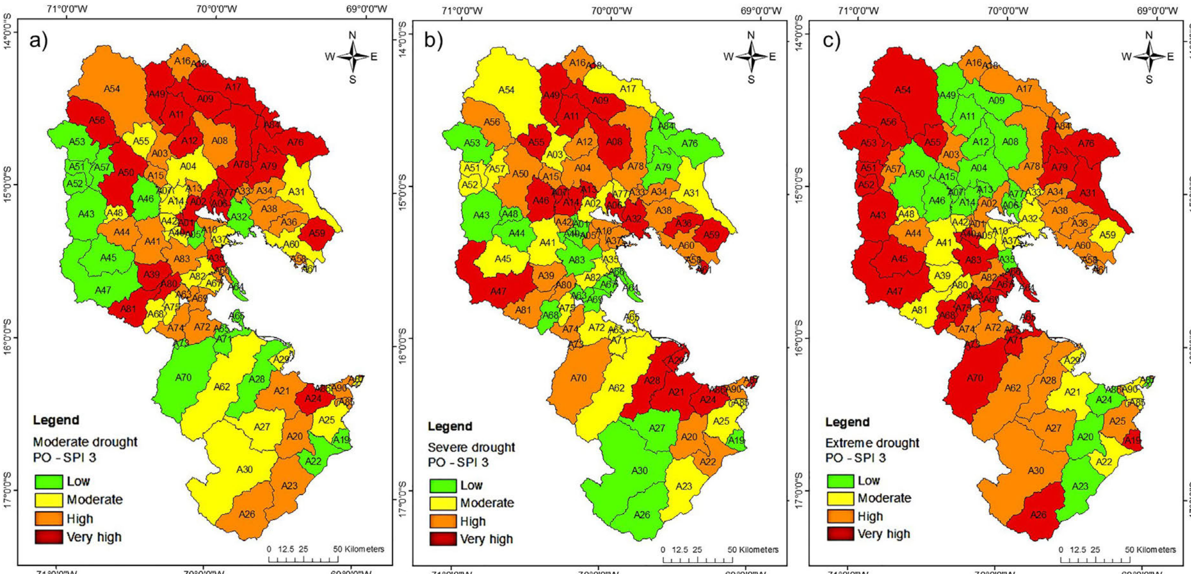

Figure 8 - The Probability of Drought Occurrence in the Titicaca Lake Basin at the district scale for a scale time of 3-months for different drought categories.

3.3. Vulnerability to drought

Figure 10 shows the vulnerability to drought of socioeconomic and physical indicators at the district scale of the Titicaca Lake Basin. The results are discussed below:

- Figure 10.a shows the population density at the district scale. The districts located in the center-east and southeast (except Pisacoma district) present high to very-high population density and cover 29% of the Basin. In this area are the districts of Juliaca and Puno that show a high population density.

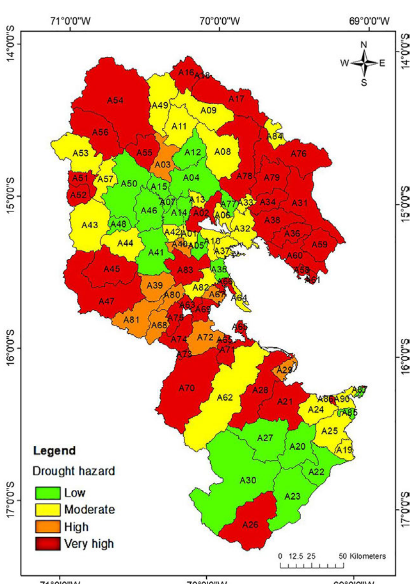

Figure 9 - Drought Hazard in the Titicaca Lake Basin at the district scale for a 3-month SPI.

- Figure 10.b shows the Economically Active Population (PEA) in the agriculture, livestock, hunting, and forestry sectors. The districts with high to very-high vulnerability are mainly located in the north, center-east, and southeast, covering 60% of the Titicaca Lake Basin. In this area are the larger territorial surface of districts such as Santa Rosa, Nuñoa and Acora.
- Figure 10.c shows the Human Development Index (IDH). The districts located in the northeast and south of the Basin have high to very-high vulnerability and occupy 43% of the area. In this zone is the Carabaya province, which according to the National Institute of Statistics and Informatics (INEI) presents a higher percentage of poverty, as the districts of Crucero and Usicayos.
- Figure 10.d shows the relationship between women and men. The districts located in the center-north have a larger population of women than men, occupying 38% of the Titicaca Lake Basin. According to the Intergovernmental Panel on Climate Change (IPCC), the climate crisis affects women more than men. The provinces with the largest number of districts within this zone are Azángaro, Carabaya, Moho, and San Román.
- Figure 10.e shows livestock production. Most of the districts of the Basin of Lake Titicaca present high to very-high livestock production, covering 80% of the Basin. According to Ardiles (2015), the Puno department is the most important in the country in terms of livestock production and the main domestic supplier of meat. The districts with the highest risk are: Acora, Ilave, Nuñoa, Santa Lucia, Santa Rosa, Juli, Pichacani, Lampa and Azángaro. In addition, the districts with the least number of livestock units are located in the eye-

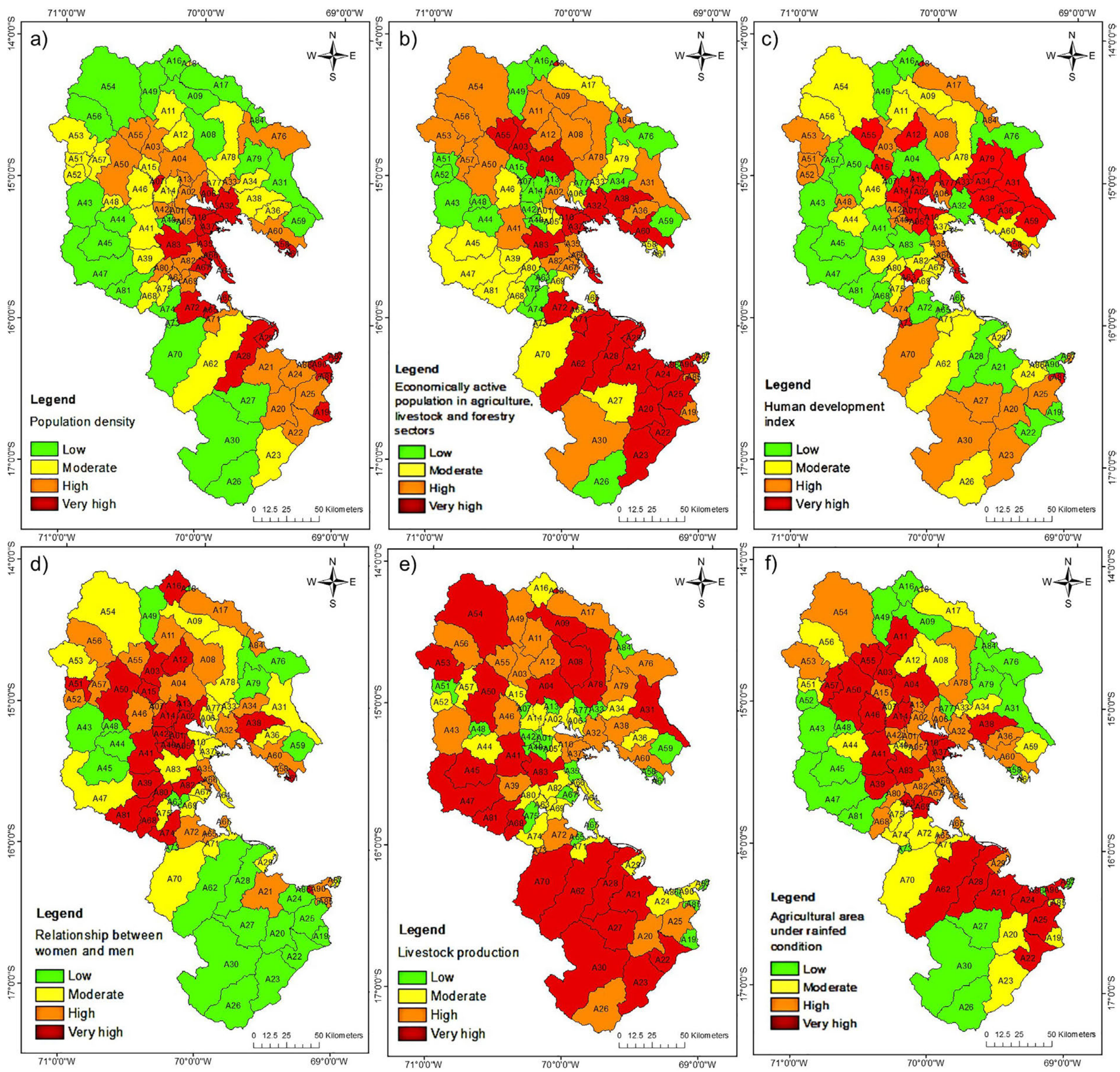

Figure 10 - Vulnerability to drought of socioeconomic and physical indicators at the district scale of the Titicaca Lake Basin.

brow of the jungle, and in the southern such as Cuturapi, Unicachi and Tinicachi.

- Figure 10.f shows the rainfed agricultural area, finding that the districts located in the center-north and southeast (except the districts of Capazo, Pisacoma, Huacullani) of the Titicaca Lake Basin, have high to very-high vulnerability to drought and occupy 45% of the area. The main provinces are Puno, Azángaro, Melgar, Chucuito, Huancané, Lampa, El Collao, and San Román.

Figure 11 shows vulnerability to drought at the district scale in the Titicaca Lake Basin. The map is divided into districts with low, moderate, high, and very-high vulnerability obtained 33 districts out of 90 (33/90) with very-high vulnerability, 13/90 districts with high vulnerability, and 22/90 with moderate vulnerability. The districts with high and very-high vulnerability are located in the center-north and southeast of the Basin, occupying 47% of the surface. The Puno region is considered the main producer of livestock in the departments of the high-Andean zone of Peru, however, still maintains levels of monetary poverty higher than the national average (Paredes and Escobar, 2018). The districts within the Titicaca Lake Basin that present high levels of poverty at the national level, higher livestock production, and depend on the agricultural sector in special rainfed agricultural are Macari, Zepita, Vilque chico, Asillo, Orurillo and Saman. In addition, in the zone of greatest vulnerability are the provinces with the highest population density as Puno, Huancané, Azángaro, San Román, and

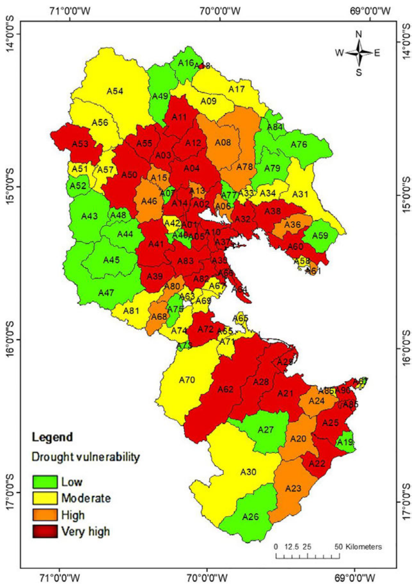

Figure 11 - Vulnerability to drought on the Titicaca Lake Basin at the district scale.

important districts such as Puno and the city of Juliaca which is considered a gigantic permanent market and is the economic capital of the department of Puno (Apaza, 2016). Likewise, the districts of Ayaviri, Muñani, Juli and Azángaro, have a larger surface extension and present more women than men. The districts with moderate to low vulnerability are located in the west, southwest, and northeast. There are areas with a low vulnerability that border areas with high or very high vulnerability, due to the socio-economic and physical indicators are independent in each district.

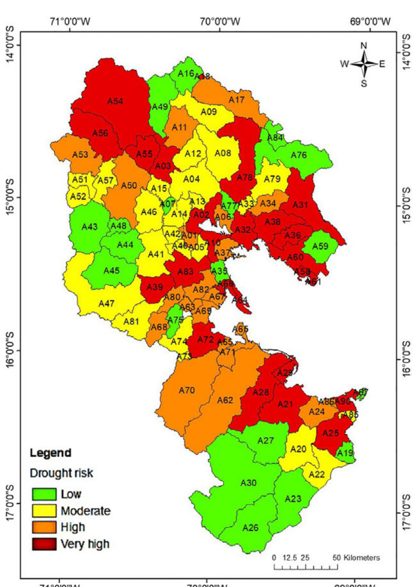

Figure 12 - Drought risk on the Titicaca Lake Basin at the district scale for a 3-month SPI.

3.4. Drought risk

Figure 12 shows the drought risk for a time scale of 3-months in the Titicaca Lake Basin at the district scale. The results show that 25 districts out of 90 (25/90) present very-high risk, 20/90 districts with high risk, and 24/90 districts with moderate risk. The districts with high and very high drought risk are localized in the northwestern, center-east, and center-south of the Titicaca Lake Basin, occupying 53% of the Basin. The districts with low to moderate drought risk are located in the zones of southern and center-western of the Basin. The provinces main with a larger number of districts in the zones with high and very-high drought risk are: Azángaro province that present one of the higher population densities and has a larger development in livestock (Romero, 2013), and inside are the districts: Achaya, Chupa, Saman, Arapa, Asillo, and San Anton. Another province is Melgar, where are the districts: Orurillo, Macari, Ayaviri, Nuñoa, and Santa Rosa. The Nuñoa district, present the second-largest district area within the Titicaca Lake Basin with high livestock production and agricultural area under rainfed. Additionally, the Carabaya province presents a higher percentage of poverty and contains the districts of Usicayos and Crucero. The Usicayos district is the second poorest district at the national level with a 96.9% incidence of poverty (INEI, 2013). The provinces that stand out the most for their economy are Puno and San Román. The San Román province has the districts: Cabana, Caracoto and Juliaca. The Puno province contain the districts: Acora, Pichacani, Puno, Mañazo, Plateria, Paucarcolla, Atuncolla, Huata, Chucuito, Capachica and Coata. The Acora district present the third-largest district area within the Titicaca Lake Basin with high livestock production and agricultural area under rainfed. The cities of Juliaca and Puno have a high population density that is 4 and 3 times higher than the departmental average, and concentrate most of the industry, commerce, as well as infrastructure, and state services of the Puno department (Ardiles, 2015). The city of Juliaca is considered as the economic capital of the department of Puno; there local, regional, national and cosmopolitan entrepreneurs compete (Apaza, 2016).

4. Conclusions

The drought hazard was estimated as the precipitation deficit monthly rainfall obtained from product PISCO-Precipitation v1.2 (Peruvian Interpolation of the SENAMHIs Climatological and Hydrological Stations) for the period 1981 to 2016 (36 years), and then was quantified with the Standardized Precipitation Index (SPI) for a time scale of 3-months. The rainy season of the Titicaca Lake Basin occurs in January, February, and March (JFM), due to that more than 50% of precipitation accumulates in these months. The rainy months in the Basin are very important because the main economic activities depend on the rains for their development. The hydrographic units of the Basin, located in the southern and eastern show negative fluctuation of precipitation, which indicates a decrease in the precipitation concerning the average, however, not show statistical significance. According to the SPI, in 1983, 1987, 1990, and 1992 in the rainy season occurred extreme, severe, and moderate drought events, with different categories and intensities. Additionally, in 1982, 1989, 1998, 2005, 2006, 2009, and 2016, were detected in some districts of the Basin severe and moderate droughts. The areas with larger predominant of drought hazard are localized in the northeast and center-south of the Titicaca Lake Basin. Our results demonstrated that precipitation deficit occurs mainly associated with the occurrence of anomalous warm SST conditions in the central Pacific rather than the eastern Pacific (Figs. 3, 7 and Table 5).

The Titicaca Lake Basin is located within the high-Andean region of the department of Puno, which is one of the departments with more poverty at the national level. The drought vulnerability varies in the districts due to the differences in socioeconomic and physical indicators, for this reason, the Basin present districts with a low vulnerability that border districts with high or very high vulnerability. The zones with high and very-high vulnerability are located in the center-north and southeast of the Basin. These zones include provinces with the highest population density, districts with the highest levels of poverty, and those economically dependent on the livestock and agricultural sectors, in special rainfed agricultural.

In the Titicaca Lake Basin was identified 45/90 districts with high to very-high risk of drought, that was obtained based on hazard and vulnerability. These districts have a large deficit of precipitation concerning the average and main socioeconomic and physical indicators vulnerable to drought hazard. The districts occupy 53% area of the Basin that are located in northwestern, center-east, and center-south. Within this area are important provinces such as Puno, San Roman, Azángaro, Melgar, and Carabaya, as well as the districts of Puno and Juliaca, the latter considered the economic capital of the department of Puno.

The Titicaca Lake Basin is the poorest region of the country with an economy that depends on precarious rainfed agriculture and an extensive and mixed livestock rearing system, so the impact of droughts generates large economic losses and increases poverty in the region, as has been recorded in the past. Therefore, based on the present study where the districts with the highest risk of droughts are identified, is important that decision-makers and the population can develop preventive measures to mitigate and reduce the impacts of the drought phenomenon in the high-Andean region of Puno.

References

ACEITUNO, P.; MONTECINOS, A. Circulation anomalies associated with dry and wet periods in the South American Altiplano. In: **Proceedings of the Fourth International Conference on Southern Hemisphere Meteorology**, Hobart: American Meteorological Society, p. 330-331, 1993.

ANA. **Las Condiciones de Sequía y Estrategias de Gestión en el Perú. Informe Nacional del Perú**. Lima: Autoridad Nacional del Agua, p. 11, 2013.

ANDRADE, M. **Atlas-Clima y eventos extremos del Altiplano Central Perú-Boliviano/Climate and extreme events from the central Altiplano of Peru and Bolivia 1981-2010**. 1 Lima: Ed. Imprenta A.G. Carrasco, p. 188, 2017.

APAZA, H. Actividades Económicas en Juliaca. **Revista de Investigación "K´uskiykuy"**, v. 1, n. 1, p. 185-194, 2016.

ARDILES, J. **PUNO: Planificación, Estrategia de Crecimiento Económico y Desarrollo Regional**. 1. ed. Puno: Universidad Nacional del Altiplano, p. 374, 2015.

AYBAR, C.; LAVADO, W.; HUERTA, A.; FERNÁNDEZ, C.; VEGA, F.; *et al*. **Uso del Producto Grillado PISCO de Precipitaciones en Estudios, Investigaciones y Sistemas Operacionales de Monitoreo y Pronostico Hidrometeorológico**. Lima: Servicio Nacional de Meteorología e Hidrología del Perú, p. 22, 2017.

CAI, W.; MCPHADEN, M.; GRIMM, A.; RODRIGUES, R.; TASCHETTO, A.; *et al*. Climate impacts of the El Niño-Southern oscillation on South America. **Nature Reviews Earth & Environment**, v. 1, p. 215-231, 2020. doi

CAVIEDES, C. Secas and El Niño: Two simultaneous climatical hazards in South America. In: **Proceedings of the Association of American Geographers**, v. 5, p. 6, 1973.

CHUCHÓN, E.; PEREIRA, A. The diurnal cycle of precipitation over Lake Titicaca Basin based on CMORPH. **Atmosphère**, v. 13, n. 4, p. 601, 2022.

CHAFFAUT, I.; POUYAUD, B.; MICHELOT, J.L.; COUDRAIN-RIBSTEIN, A. Précipitations d'altitude du Nord-Chili, origine des sources de vapeur et données isotopiques. **Bulletin de l'Institut Française d'Etudes Andines**, v. 27, n. 3, p. 367-384, 1998.

CLAVERÍAS, R. **El Desarrollo Sostenible en la Cultura Andina**. 1. ed. Puno: Universidad Nacional del Altiplano, p. 269, 2016.

ENDARA, S. **Determinación de Extremos a Precipitación a Partir del PISCO Diario**. Lima: Servicio Nacional de Meteorología e Hidrología del Perú, 83 p., 2017.

ENDARA, S.; ACUÑA, J.; VEGA, F.; FEBRE, C.; CORREA, K; *et al*. **Caracterización Espacio Temporal de la Sequía en los Departamentos Altoandinos del Perú (1981-2018)**. Lima: Servicio Nacional de Meteorología e Hidrología del Perú, p. 31, 2019.

GARREAUD, R.; VUILLE, M.; CLEMENT, A. The climate of the Altiplano: Observed current conditions and mechanisms of past changes. **Palaeogeography, Palaeoclimatology, Palaeoecology**, v. 194, p. 5-22, 2003.

GUTTMAN, N. Comparing the palmer drought index and the standardized precipitation index. **Journal of the American Water Resources Association**, v. 34, n. 1, p. 113-121,1998.

YOUNG-SIK, M.; WON-HO, N.; MIN-GI, J.; NA-KYOUNG, B.; TAEGON, K. Assessment of vulnerability to drought disaster in agricultural reservoirs in South Korea. **Journal Atmosphere**, v. 11, n. 11, p. 1244, 2020.

HUNGGSOO, K.; JONGYONG, P.; JIYOUNG, Y.; TAE-WOONG, K. Assessment of drought hazard, vulnerability, and risk: A case study for administrative districts in South Korea. **Journal of Hydro-environment Research**, v. 9, n. 1, p. 28-35, 2015.

IMFELD, N.; BARRETO, C.; COOREA, K.; JACQUES-COPER, M.; SEDLMEIER, K.; *et al*. Summertime precipitation deficits in the southern Peruvian highlands since 1964. **International Journal of Climatology**, v. 39, p. 4497-4513, 2019.

INDECI. **Boletín Estadístico Virtual de la Gestión Reactiva del INDECI (Nº 01)**. Lima: Indeci, p. 32. 2014.

INEI. **IV Censo Nacional Agropecuario 2012: PUNO Perfil Agropecuario**. Punto: Grafia S.A.C., p. 201, 2013.

JOHNSON, K.; DEPIETRI, Y.; BREIL, M. Multi-hazard risk assessment of two Hong Kong districts. **International Journal of Disaster Risk Reduction**, v. 19, p. 311-323, 2016. doi

LAGOS, P.; SILVA, Y.; NICKL, E.; MOSQUERA, K. El Niño related precipitation variability in Perú. **Advances in Geosciences**, v. 14, p. 231-237, 2008. doi

LAVADO, W.; JOSYANE, D.; ESPINOZA, J.C.; LOUP, J. Basin-scale analysis of rainfall and runoff in Peru (1969-2004): Pacific, Titicaca and Amazonas drainages. **Hydrological Sciences Journal**, v. 57, n. 4, p. 625-642, 2012.

LAVADO, W.; ESPINOZA, J.C. Impactos de El Niño y La Niña en las lluvias del Perú (1965-2007).**Revista Brasileira de Meteorologia,** v. 29, n. 2, p 171-182, 2014.

LOVÓN, G. **El Sur Andino Peruano y la Coyuntura de Sequía: 1982-1983**. Buenos Aires: Grupo Editor Latinoamericano, p. 17, 1985.

MAYTA, V.; AMBRIZZI, T.; ESPINOZA, J.C.; SILVA, P. The role of the Madden-Julian oscillation on the Amazon Basin intraseasonal rainfall variability. **International Journal of Climatology**, v. 39, n. 1, p. 343-360, 2019.

MCKEE, T.; DOESKEN, N.; KLEIST, J. The Relationship of drought frequency and duration to time scales. In: **Eighth Conference on Applied Climatology**, Anaheim, p. 17-22, 1993.

OMM. **Vigilancia y Alerta Temprana de la Sequía: Conceptos, Progresos y Desafíos Futuros (OMM-Nº 1006)**. Geneva: Organización Meteorológica Mundial, p. 28, 2006.

OMM. **Guía del usuario sobre el Índice normalizado de precipitación (OMM-Nº 1090)**. Geneva: Organización Meteorológica Mundial, p. 23, 2012.

ORTEGA, D. Sequía: Causas y efectos de un fenómeno global. **Ciencia UANL**, n. 61, p. 9, 2013.

ORTLIEB, L.; MACHARÉ, J. Former El Niño events: records from western South America. **Global and Planetary Change**, v. 7, n. 1-3, p. 181-202, 1993.

PAREDES, R.; ESCOBAR, F. El rol de la ganadería y la pobreza en el área rural de Puno. **Journal of High Andean Research**, v. 20, n. 1, p. 39-60, 2018.

PORTO, A. **Validación del Producto Grillado Pisco de Precipitación v2.1 con la Data Observada de las Estaciones Pluviométricas del SENAMHI en la Cuenca de la Vertiente del Lago Titicaca - Lado Peruano**. Puno: Universidad Nacional del Altiplano, 2021.

ROJAS, O. Next Generation Agricultural Stress Index System (ASIS) for agricultural drought monitoring. **Remote Sens**, v. 13, n. 5, p. 959, 2021.

ROMERO, E. **Monografía del Departamento de Puno**. 3. ed. Puno: Universidad Nacional del Altiplano, p. 601, 2013.

SERAFINI, B.; OLIVEIRA-JÚNIOR, J.; DE GOIS, G.; PEREIRA-JÚNIOR, E. Drought characterization for the state of Rio de Janeiro based on the annual SPI index: trends, statistical tests and its relation with ENSO. **Atmospheric Research**, v. 220, p. 141-154, 2019.

SMITH, R. Comparing traditional methods for selecting class intervals on choropleth maps. **The Professional Geographer**, v. 38, n. 1, p. 62-67, 1986.

SÖNMEZ, K.; KÖMÜSCÜ, A.; ERKAN, A.; TURGU, E. An analysis of spatial and temporal dimension of drought vulnerability in Turkey using the standardized precipitation index. **Natural Hazards**, v. 35, n. 2, p. 243-264, 2005.

SHAHID, S.; BEHRAWAN, H. Drought risk assessment in the western part of Bangladesh. **Natural Hazards**, v. 46, n. 3, p. 391-413, 2008.

SULCA, J.; TAKAHASHI, K.; ESPINOZA, J.C.; VUILLE, M.; LAVADO-CASIMIRO, W. Impacts of different ENSO flavors and tropical Pacific convection variability (ITCZ, SPCZ) on austral summer rainfall in South America, with a focus on Peru. **International Journal of Climatology**, v. 38, n. 1, p. 420-435, 2018.

TAKAHASHI, K.; MONTECINOS, A.; GOUBANOVA, K.; DEWITTE, B. ENSO regimes: Reinterpreting the Canonical and Modoki El Niño. **Geophysical Research Letters**, v. 38, n. 10, p. 5, 2011.

TANNEHILL, I. Drought, its causes and effects, Princeton, NJ: Princeton University Press. **American Journal of Agricultural Economics**, v. 29, n. 3, p. 779-781, 1947.

VEGA, F. **Análisis del Riesgo de Sequias en el Sur del Perú**. Lima: Servicio Nacional de Meteorología e Hidrología del Perú, 2016.

VERA, C.; HIGGINS, W.; AMADOR, J.; AMBRIZZI, T.; GARREAUD, R.; *et al.* Toward a unifed view of the American monsoon systems. **Journal of Climate**, v. 19, n. 20, p. 4977-5000, 2006.

VIZY, E.; COOK, K. Relationship between Amazon and high Andes rainfall. **Journal of Geophysical Research-Atmospheres**, v. 112, n. 7, p. 14, 2007.

VUILLE, M.; DOUGLAS, H.; CARSTEN, F.; RAYMOND, B. Atmospheric circulation anomalies associated with 1996/1997 summer precipitation events on Sajama Ice Cap, Bolivia. **Journal of Geophysical Research-Atmospheres**, v. 103, n. 10, p. 11191-11204, 1998.

WILHITE, D.A. Drought as a natural hazard: Concepts and definitions. **Published in Drought: A Global Assessment**, v. I, p. 3-18, 2000.

WMO. **Handbook of Drought Indicators and Indices. Integrated Drought Management Programme (IDMP), Integrated Drought Management Tools and Guidelines Series 2**. Geneva: WMO, p. 52, 2016.

ZHOU, J.; LAU, K.M. Does a Monsoon climate exist over South America? **Journal of Climate**, v. 11, n. 5, p. 1020-1040, 1998.

Internet Resources

Census population, statistical information of Economically Active Population, https://www.inei.gob.pe/media/MenuRecursivo/publicaciones_digitales/Est/Lib1627/.

Climate Monitoring Indices of the Geophysical Institute of Peru, http://met.igp.gob.pe/variabclim/indices.html.

Human Development Index, https://www.pe.undp.org/content/peru/es/home/library/poverty/Informesobredesarrollohumano2013/IDHPeru2013/.

National Censuses 2017: Population XII, Housing VII, and Indigenous Communities III, https://www.inei.gob.pe/media/MenuRecursivo/publicaciones_digitales/Est/Lib1541/index.htm

NOAA Climate Indices, https://psl.noaa.gov/data/climateindices/list/.

SENAMHI, http://www.senamhi.gob.pe.

License information: This is an open-access article distributed under the terms of the Creative Commons Attribution License (type CC-BY), which permits unrestricted use, distribution and reproduction in any medium, provided the original article is properly cited.